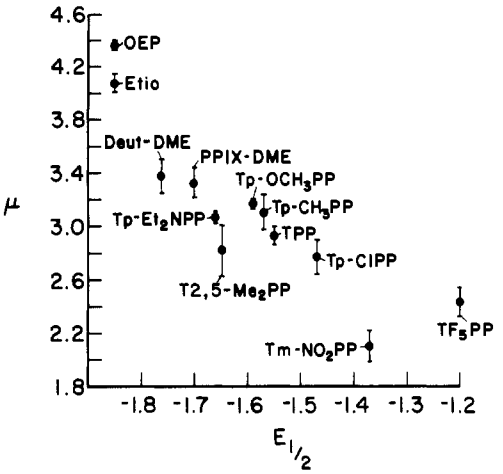

Figure 2. Magnetic moments of $[Fe(Porph)(3\text{-}Cl(py))_2]ClO_4$ in 30% 3-chloropyridine in nitromethane.

A Varian EM-390 NMR spectrometer with a probe temperature of 35 °C was employed. At least three independent measurements were made for each complex. Diamagnetic corrections were applied to all molar susceptibilities and were calculated by direct summations of individual constants[24] or by adding appropriate corrections to the values reported for the free-base porphyrin.[25]

The magnetic moments for the various $[Fe(Porph)(3\text{-}Cl(py))_2]ClO_4$ complexes examined range from 2.0 to 4.4 μ_B and are given in Table I.[26] The results indicate that the porphinato ligand significantly influences the magnetic moment. A reasonable, although not unique, interpretation is that the porphinato ligand affects the amount of the $S = {}^5/_2$ component in an $S = {}^1/_2$, $S = {}^5/_2$ thermal spin equilibrium. The effect of the porphinato ligand on metalloporphyrin chemistry has recently been reviewed.[27] These "cis" effects change redox properties[28] and axial-ligand binding constants[29] and follow Hammet relationships.

The magnetic moment of $[Fe(OEP)(X\text{-}py)_2]ClO_4$ complexes have been shown to be sensitive to the pyridine substituent.[12] A decrease in pyridine basicity results in an increase in high-spin fraction for these $S = {}^1/_2$, $S {}^5/_2$ systems. The results presented herein show a dependence on the porphinato-ligand basicity as well. Although direct measurements of porphinato basicity are not available for all species, Hambright et al.[30] have recently compiled extensive lists of half-wave reduction potentials for free-base porphyrins. The reduction potential has been shown to be a good measure of the porphyrin basicity. A linear relationship between these potentials and porphyrin pK_a's has been shown to exist.[30a] A plot of the half-wave reduction potentials of the free-base porphyrins vs. the magnetic moments of the $[Fe(Porph)(3\text{-}Cl(py))_2]ClO_4$ complexes shows the moments to be qualitatively dependent on porphyrin basicity (see Figures 1 and 2). A decrease in the high-spin fraction from approximately 50% to nearly zero is observed as the basicity of the porphyrin decreases.

A possible explanation for the observed porphinato-ligand effect on spin state comes from consideration of a simple charge-attraction model.[7a] The more basic porphyrins donate more electron density to the iron(III) atom and thus decrease its charge attraction for the axial ligands. This results in a decrease of the axial-ligand field, which is known[4] to lead to higher spin multiplicity.

Acknowledgment. The support of the National Institutes of Health (Grant HL-15627) is gratefully acknowledged.

Registry No. $[Fe(OEP)(3\text{-}Cl(py))_2]ClO_4$, 71414-31-8; $[Fe(Etio)(3\text{-}Cl(py))_2]ClO_4$, 89936-65-2; $[Fe(Deut\text{-}DME)(3\text{-}Cl(py))_2]ClO_4$, 89936-67-4; $[Fe(PPIX\text{-}DME)(3\text{-}Cl(py))_2]ClO_4$, 89936-69-6; $[Fe(T\text{-}p\text{-}Et_2NPP)(3\text{-}Cl(py))_2]ClO_4$, 89936-71-0; $[Fe(T\text{-}2,5\text{-}Me_2PP)(3\text{-}Cl(py))_2]ClO_4$, 89936-73-2; $[Fe(T\text{-}p\text{-}OCH_3PP)(3\text{-}Cl(py))_2]ClO_4$, 89936-75-4; $[Fe(T\text{-}p\text{-}CH_3PP)(3\text{-}Cl(py))_2]ClO_4$, 89936-77-6; $[Fe(TPP)(3\text{-}Cl(py))_2]ClO_4$, 72318-32-2; $[Fe(T\text{-}p\text{-}ClPP)(3\text{-}Cl(py))_2]ClO_4$, 89936-79-8; $[Fe(T\text{-}m\text{-}NO_2PP)(3\text{-}Cl(py))_2]ClO_4$, 89936-81-2; $[Fe(TF_5PP)(3\text{-}Cl(py))_2]ClO_4$, 89936-83-4.

(21) The large excess of axial ligand employed in the measurements ensures that the observed species is six-coordinate. The equilibrium constant for the addition of the second axial ligand to iron porphyrins has been reported to be greater than that of the first for imidazole[22] and pyridine[23] complexes (log β_2 = 6.7 for the addition of 3-Cl(py) to Fe(TPP)-$(OClO_3)$).[23a] Furthermore, β_2's increase[22] with increasingly basic porphinates, making it unlikely that the complexes with higher magnetic moments are five-coordinate.

(22) Walker, F. A.; Lo, M.-W.; Ree, M. T. *J. Am. Chem. Soc.* **1975**, *97*, 5552–5560.

(23) (a) Kadish, K. M.; Bottomley, L. A. *Inorg. Chem.* **1980**, *19*, 832–836. (b) Yoshimura, T.; Osaki, T. *Bull. Chem. Soc. Jpn.* **1979**, *52*, 2268–2275 and references therein. (c) Coyle, C. L.; Rafson, P. A.; Abbott, E. H. *Inorg. Chem.* **1973**, *12*, 2007–2010. (d) Burdige, D.; Sweigart, D. A. *Inorg. Chim. Acta* **1978**, *28*, L131–L132 and references therein.

(24) Mulay, L. N. In "Physical Methods of Chemistry"; Weissburger, A., Rossiter, B. W., Eds.; Wiley-Interscience: New York, 1972; Vol. I, part IV.

(25) Eaton, S. S.; Eaton, G. R. *Inorg. Chem.* **1980**, *19*, 1095–1096.

(26) We have no explanation for the variations in magnetic moment of a *given* complex with solvent. We do note that for $[Fe(OEP)(3\text{-}Cl(py))_2]ClO_4$ reproducible differences in solution susceptibilities exist even for solvents as similar as methylene chloride and chloroform (Skyte, P. D. Thesis, University of Oxford, 1977. Geiger, D. K. Ph.D. Thesis, University of Notre Dame, 1983). Solvent dependence for solution magnetic moments of N_4O_2 iron(III) complexes have also been reported: Dose, E. V.; Murphy, K. M. M.; Wilson, L. J. *Inorg. Chem.* **1976**, *15*, 2622–2630.

(27) Buchler, J. W.; Kokisch, W.; Smith, P. D. *Struct. Bonding (Berlin)* **1978**, *34*, 79–134.

(28) Kadish, K. M.; Morrison, M. M. *Bioinorg. Chem.* **1977**, *7*, 107–115. Walker, F. A.; Beroiz, D.; Kadish, K. M. *J. Am. Chem. Soc.* **1976**, *98*, 3484–3489.

(29) Kadish, K. M.; Shiue, L. R. *Inorg. Chem.* **1982**, *21*, 1112–1115. Kadish. K. M.; Bottomley, L. A.; Beroiz, D. *Ibid. Chem.* **1978**, *17*, 1124–1129. Saterlee, J. D.; LaMar, G. N.; Frye, J. S. *J. Am. Chem. Soc.* **1976**, *98*, 7275–7282. Walker, F. A.; Lo, M.-W.; Ree, M. T. *Ibid.* **1976**, *98*, 5552–5560. Walker, F. A.; Hui, E.; Walker, J. M. *Ibid.* **1975**, *97*, 2390–2397.

(30) (a) Worthington, P.; Hambright, P.; Williams, R. F. X.; Feldman, M. R. *Inorg. Nucl. Chem. Lett.* **1980**, *16*, 441–447. (b) Worthington, P.; Hambright, P.; Williams, R. F. X.; Reid, J.; Burnham, C.; Shamin, A.; Turay J.; Bell, D. M.; Kirkland, R.; Little, F. G.; Datta-Gupta, N.; Eisner, U. *J. Inorg. Biochem.* **1980**, *12*, 281–291. (c) Williams, R. F. X.; Hambright, P. *Bioinorg. Chem.* **1978**, *9*, 537–544.

Contribution from the Departments of Chemistry, Oregon State University, Corvallis, Oregon 97331, and University of California at Davis, Davis, California 95616

Molecular Structure of Bis[bis(trimethylsilyl)amido]zinc As Determined by Gas Electron Diffraction

Arne Haaland,[1a] Kenneth Hedberg,*[1b] and Philip P. Power[1c]

Received August 11, 1983

The synthesis of bis[bis(trimethylsilyl)amido]zinc was first reported by Bürger and co-workers in 1965.[2,3] These authors found the infrared and Raman spectra to be consistent with planar $ZnNSi_2$ fragments and collinear bonds from Zn to the nitrogen atoms, but no conclusions could be drawn about the

(1) (a) Oregon State University. Present address: University of Oslo, Oslo, Norway. (b) Oregon State University. (c) University of California at Davis.

(2) Bürger, H.; Sawodny, W.; Wannagat, U. *J. Organomet. Chem.* **1965**, *3*, 113.

(3) For a recent review of metal amides see: Lappert, M. F.; Power, P. P.; Sanger, A. R.; Shrivastava, R. C. "Metal and Metalloid Amides"; Ellis Harwood: Chichester, England, 1980.

0020-1669/84/1323-1972$01.50/0

Table I. Results for $[(Me_3Si)_2N]_2Zn$[a,b]

defining parameters	r_a or ∠	l	nondefining parameters	r_a or ∠	l
Zn-N/Å	1.824 (14)	0.042 (25)	Zn·Si/Å	2.992 (12)	0.11 (5)
N-Si/Å	1.728 (7)	[0.057]	Si·Si/Å	3.14 (3)	[0.082]
Si-C/Å	1.889 (6)	[0.062]	N·C/Å	3.03 (3)	[0.098]
C-H/Å	1.105 (4)	0.083 (5)	C·C/Å	3.00 (4)	[0.113]
∠Zn-N-Si/deg	114.8 (10)		Si·H/Å	2.51 (1)	0.130 (10)
∠N-Si-C/deg	113.5 (20)		Zn· ·C/Å	3.30-4.54	[0.15-0.30]
∠Si-C-H/deg	111.1 (2)		Si· ·C/Å	3.77-4.70	[0.16-0.22]
τ(Si-N)/deg	20 (6)		N· ·N/Å	3.65 (3)	[0.080]
V_2/kcal·mol^{-1}	2.5 (10)		N· ·Si/Å	4.64 (2)	0.123 (25)
			Si· · ·Si/Å	5.56 (3)	[0.123][c]
			Si· · ·C/Å	5.1-7.2	[0.17][c]
			∠Si-N-Si/deg	130.4 (20)	
			R[d]	0.0416	

[a] Parenthesized uncertainties are estimates of 2σ. They have been expanded to include uncertainties in nonrefined amplitudes. [b] Quantities in square brackets were assumed. [c] Framework value; see text. [d] $R = [\Sigma w_i[sI(\text{obsd}) - sI(\text{calcd})]_i^2/\Sigma w_i[sI(\text{obsd})]_i^2]^{1/2}$.

relative orientation of the NSi_2 groups (coplanar, symmetry D_{2h}; or staggered, D_{2d}). More recently, the molecular structure of the beryllium analogue, $[(Me_3Si)_2N]_2Be$, has been determined by gas electron diffraction (GED) and the $Si_2NBeNSi_2$ backbone found to be staggered.[4] The allene-like equilibrium conformation was attributed to dative $p\pi$–$p\pi$ bonding between the nitrogen atoms and the metal; no attempt was made to determine the rotational barrier. In this note we present the results of a GED investigation of $[(Me_3Si)_2N]_2Zn$. As in the beryllium compound, the equilibrium conformation is found to be staggered. The barrier to internal rotation about the NZnN axis is found to be 2.5 (1.5) kcal·mol^{-1}.

Experimental Section

A sample of $[(Me_3Si)_2N]Zn$ was synthesized in the manner described by Bürger and co-workers.[2]

Diffraction photographs were made in the Oregon State apparatus with an r^3 sector and nozzle-to-plate distances of about 748 and 301 mm. The nozzle temperature was 115–120 °C and the reservoir temperature about 10 °C lower. Five plates from each distance were photometered and the data processed by the standard procedures of this laboratory. Data for the leveled total intensities ($s^4I_t(s)$), final backgrounds, and average molecular intensities ($sI_m(s)$) are available as supplementary material; curves of these data are shown in Figure 1.

Structure Refinement

The first least-squares refinements were based on a model with a staggered $Si_2NZnNSi_2$ backbone in which the Me_3Si groups were oriented to give overall S_4 symmetry as indicated in Figure 2. It was assumed that (i) the $SiCH_3$ fratgments have C_{3v} symmetry, (ii) the orientation of the methyl groups is such that one C–H bond is anti to the adjacent Si–N bond, and (iii) the $NSiMe_3$ fragments have C_{3v} symmetry. Although arbitrary, and in a strict sense certainly not true in the first and last cases, these assumptions in no way limit the validity of our principal results. The molecular structure is then determined by eight parameters, e.g., the Zn–N, N–Si, Si–C, and C–H bond distances, the Zn–N–Si, N–Si–C, and Si–C–H bond angles, and the angle of twist of the Me_3Si groups about the Si–N bond, τ(Si–N). This angle we define as zero when one Si–C bond is anti the adjacent N–Si bond.

The molecule is too large and the symmetry too low to allow refinement of all vibrational amplitudes. The amplitudes of interatomic distances within each $(Me_3Si)_2N$ ligand were therefore fixed at values similar to those determined for $(Me_3Si)_2NH$ from electron diffraction and force-field calculations by Fjeldberg and co-workers.[5] Terms corresponding to distances between carbon atoms at different ends of the molecule, i.e., in different $N(SiMe_3)_2$ groups, were omitted from the calculated intensities: these distances are distributed over a very large range (about 5.0–9.0 Å) and tend to be quickly damped out by large-amplitude vibration. Vibrational corrections to the distances (shrinkage) were omitted. Refinement of the eight structure parameters described above and the five vibrational amplitude parameters gave values similar to those listed in Table I.

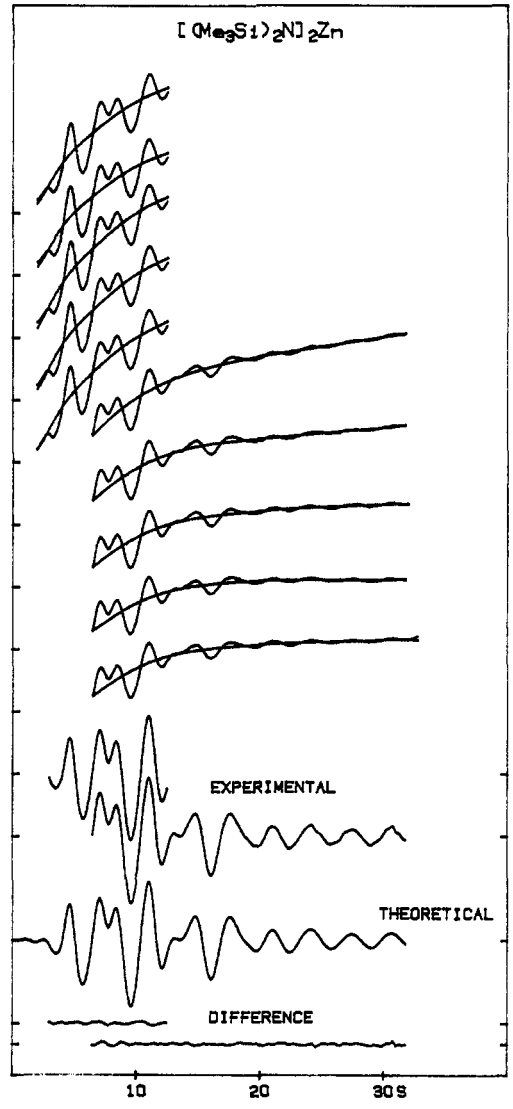

Figure 1. Intensity curves. Above: Experimental total intensity curves, s^4I_t, of single plates with final backgrounds. Below: Average experimental molecular intensity curves (s^4I_t minus background times s) and the theoretical counterpart calculated for the best model. Difference curves are experimental minus theoretical.

The large value obtained for interligand Si···Si vibrational amplitude, l = 0.24 (2) Å, suggests that the ligands undergo large amplitude libration about the NZnN axis. We therefore carried out a second set of least-squares refinements in which this motion of the molecule

(4) Clark, A. H.; Haaland, A. *Acta Chem. Scand.* **1970**, *24*, 3024.
(5) Fjeldberg, T. *J. Mol. Struct.* **1984**, *112*, 159.

Table II. Correlation Matrix (×100) for Refinement of $[(Me_3Si)_2N]_2Zn$

parameter	σ_{LS}[a]	r_1	r_2	r_3	r_4	$\angle_1$	$\angle_2$	$\angle_3$	τ	V_2	l_1	l_2	l_3	l_4	l_5
r(C-H)	0.14	100	−2	−7	−1	26	−4	5	2	−1	<1	−5	6	−6	1
r(Si-C)	0.12		100	−40	−69	31	−5	2	14	4	−88	6	16	7	12
r(N-Si)	0.11			100	30	−15	25	−37	−6	3	59	−7	−58	17	−3
r(Zn-N)	0.15				100	−17	5	−36	−10	−2	58	−14	−25	3	−9
∠SiCH	0.46					100	−15	−2	23	6	−30	−6	25	−6	13
∠NSiC	63						100	−30	32	9	9	−4	−71	−16	1
∠ZnNSi	8.6							100	−6	−8	−12	6	49	5	−5
τ(N-Si)	198								100	44	−11	4	24	6	72
V_2	24									100	−2	3	−4	1	43
l(Zn-N)	0.38										100	−3	−26	2	−9
l(C-H)	0.13											100	13	9	3
l(Zn·Si)	0.22												100	−3	4
l(Si·H)	0.29													100	1
l(N···Si)	0.98														100

[a] Standard deviations from least-squares refinement (×100). Distances and amplitudes in angstroms; angles in degrees.

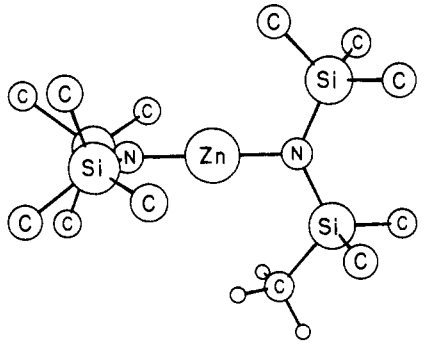

Figure 2. Molecular model of $[(Me_3Si)_2N]_2Zn$. Most of the hydrogen atoms have been omitted for clarity. The symmetry of the $Si_2NZnNSi_2$ backbone is D_{2d}, but the presence of the methyl groups lowers the symmetry to S_4.

was modeled by a mixture of seven pseudoconformers differing only in the angle between the two NSi_2 planes; this angle was assigned values from 0 to 90° in steps of 15°. The rotational potential was assumed to have the form $V(\phi) = (V_2/2)(1 + \cos 2\phi)$, and each pseudoconformer was given a weight proportional to $\exp[-V(\phi)/RT]$. The "framework" vibrational amplitude of the interligand Si···Si distances was fixed at 0.12 Å, i.e., the value obtained for the interligand N···Si distance.

Least-squares refinement of V_2, the eight structure parameters, and the four vibrational amplitudes yielded the values listed in Table I. None of the structure parameters changed perceptibly from the previous values, and the fit was only marginally improved. The theoretical intensity corresponding to the model of Table I is shown in Figure 1, and a correlation matrix is given in Table II.

Discussion

An experimental radial distribution curve is shown in Figure 3. The presence of a distinct—though broad—peak at r = 5.5 Å, corresponding to four interligand Si···Si distances, confirms that the equilibrium conformation is one in which the NSi_2 planes are staggered. (This peak would be split into two much smaller ones at about 5.1 and 6.0 Å if the backbone were planar.) The structure of $[(Me_3Si)_2N]_2Zn$ is therefore similar to that of the beryllium analogue.[4] Comparison of bond distances and valence angles reveals no significant differences between the ligands in the two compounds. (In the Be compound the values are r(Be–N) = 1.562 (24) Å, r(Si–N) = 1.722 (7) Å, r(Si–C) = 1.876 (4) Å, ∠BeNSi = 115.4 (4)°, ∠SiNSi = 129.2 (7)°, and ∠NSiC = 109.8 (9)°; numbers in parentheses are estimated standard deviations.) The torsional angle τ(N–Si), however, is larger in the Zn compound, 20 (2)° vs. 7.2 (3.5)°, probably as a consequence of greater steric interaction between methyl groups and the zinc atom. For example, the sum of the van der Waals radii for a methyl group and zinc is about 3.3 Å and for a methyl group and beryllium about 2.9 Å. If the M–N and one of the Si–C bonds

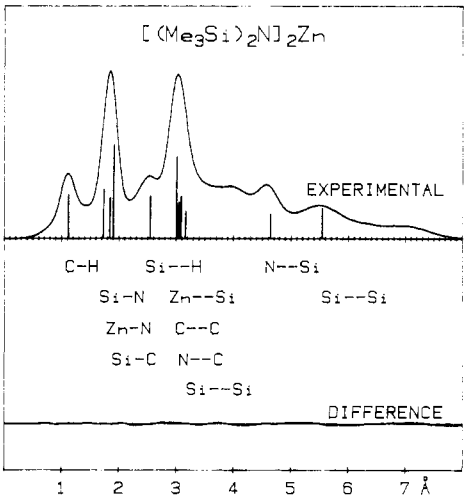

Figure 3. Above: Experimental radial-distribution curve calculated with artificial damping constant B = 0.0025 Å^2. Major interatomic peaks are indicated by vertical lines of height approximately equal to the area of the corresponding peak component. Below: Difference between the experimental radial-distribution curve and the theoretial counterpart calculated for the best model.

were to be eclipsed (τ(N–Si) = 0°), the M···C distance would be about 3.3 Å for the zinc compound and about 3.1 Å for the beryllium, suggesting greater repulsive interaction for the former. The measured values of τ(N–Si) lead to M···C distances of 3.35 Å for the zinc compound and 3.05 Å for the beryllium, corresponding to approximately equal van der Waals repulsion.

The barrier to internal rotation of the ligands in the zinc compound, V_2 = 2.5 (1.5) kcal·mol^{-1}, confirms that the molecule undergoes large-amplitude libration about a staggered equilibrium conformation; at the temperature of our experiment (390 K), it corresponds to an rms torsional amplitude of 23° (20° at room temperature). In the harmonic approximation a barrier of 2.5 kcal·mol^{-1} corresponds to a torsional normal mode with frequency ν = 13 cm^{-1}.

The barrier to internal rotation may be attributed to electronic effects (dative π-bonding), to van der Waals interaction between the two ligands, or to a combination of the two. Since the shortest distance between carbon atoms in different ligands is reduced from about 5.0 to 2.8 Å when the ligands are rotated rigidly from the staggered into the eclipsed conformation, it seems likely that a significant part of the barrier is of steric origin.

We conclude that dative π-bonding between Zn and N is relatively insignificant. This is in agreement with the view of Bürger and co-workers,[2] who felt that the magnitude of the Zn–N stretching force constant (2.24 mdyn/Å) indicates that

the Zn–N bond is a "single covalent" bond. It is also consistent with the photoelectron spectrum, which shows that the two electron pairs on the N atoms are at least approximately degenerate.[6]

Acknowledgment. This work was supported by the National Science Foundation under Grant CHE 81-10541.

Registry No. $[(Me_3Si)_2N]_2Zn$, 3999-27-7.

Supplementary Material Available: Tables of the leveled total intensities, final backgrounds, and averaged molecular intensities (11 pages). Ordering information is given on any current masthead page.

(6) Harris, D. H.; Lappert, M. F.; Pedley, J. B.; Sharp, G. J. *J. Chem. Soc., Dalton Trans.* **1976**, 945.

Contribution from the Department of Chemistry, McMaster University, Hamilton, Ontario, Canada L8S 4M1

A ^{77}Se and ^{125}Te NMR Study of the $Te_2Se_6^{2+}$ Cation: Magnetic Inequivalence of Heavy Nuclei

Michael J. Collins and Ronald J. Gillespie*

Received September 13, 1983

Selenium-77 NMR spectra were observed by us by continuous-wave methods as early as 1965.[1] In recent years developments in FT NMR spectroscopy and the availability of high-field instruments have led to a very considerable increase in studies of the NMR spectra of relatively insensitive nuclei such as ^{77}Se and ^{125}Te. Results obtained with these two nuclei have been reviewed in two recent monographs.[2,3] We have been engaged in a study of polyatomic cations of group 6 and have recently used ^{77}Se and ^{125}Te NMR spectroscopy to obtain structural information on some of these species.[4-10] (^{77}Se: spin $^1/_2$, 7.50% natural abundance, 6.9×10^{-3} relative sensitivity to ^1H. ^{125}Te: spin $^1/_2$, 7.00% natural abundance, 3.2×10^{-2} relative sensitivity to ^1H.) The present note is concerned with the $Te_2Se_6^{2+}$ cation.

The solid-state structure of the $Te_2Se_6^{2+}$ cation has recently been determined[11] in the compound $(Te_2Se_6)(Te_2Se_8)(AsF_6)_4(SO_2)_2$. The structure of this cation can be derived from a cube with the two tellurium atoms at opposite corners (Figure 1). In this structure both tellurium atoms are chemically equivalent, as are the six selenium atoms. The solid-state structure of the isovalent Se_8^{2+} cation is quite different from that of $Te_2Se_6^{2+}$. It is an eight-membered ring in the exo–endo conformation with a long transannular bond.[12] The ^{77}Se NMR spectrum of this species in SO_2 or 100% H_2SO_4 solution is consistent with this same structure.[13] The aim of the present work was to record the ^{77}Se and ^{125}Te NMR spectra of the $Te_2Se_6^{2+}$ cation to determine if the solid-state structure is retained in solution and to determine the chemical shifts and coupling constants in this species.

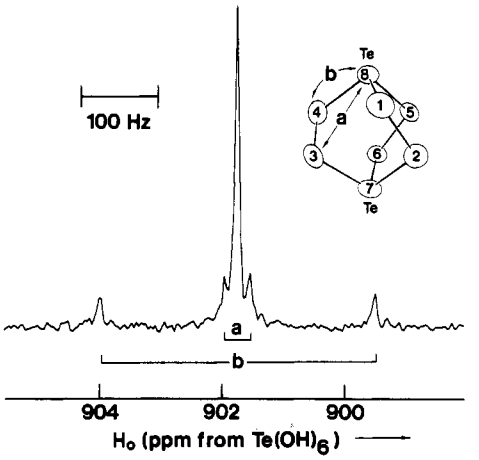

Figure 1. ^{125}Te NMR spectrum of $Te_2Se_6^{2+}$, natural abundance, showing the main resonance with two doublets corresponding to $J(^{77}Se-^{125}Te) = 355$ Hz and $^2J(^{77}Se-^{125}Te) = 32$ Hz; 148 000 scans (13.5 h), 3.0 Hz/data point. A line broadening of 1 Hz was applied to the exponential smoothing of the free-induction decay.

Experimental Section

Materials. Elemental selenium and tellurium (Koch-Light Laboratories Ltd.) were dried overnight at 24 °C on a vacuum line. Tellurium enriched to 77.3% ^{125}Te was obtained by reduction of the enriched dioxide[14] (Techsnabexport, Moscow). $(Te_2Se_8)(AsF_6)_2(SO_2)$ and $(Te_2Se_8)(AsF_6)_2$ were prepared as previously described.[5,11] Arsenic pentafluoride and arsenic trifluoride were prepared from the elements on a Monel vacuum line. AsF_5 was stored in a Monel cylinder; AsF_3 in a nickel pot over sodium fluoride. A sample of 100% H_2SO_4 was prepared by combining 96% H_2SO_4 and 30% oleum (Fisher Scientific Co.) until a maximum freezing point was obtained.

Sample 1. A sample of 200 mg of $(Te_2Se_8)(AsF_6)_2(SO_2)$ was transferred in a drybox into a 10-mm o.d. precision glass NMR tube (Wilmad) joined to $^1/_4$-in. o.d. standard wall tubing. The sample tube was attached to a vacuum line by means of a Teflon valve, and 5 g of AsF_3 was distilled into the tube at −196 °C before flame sealing.

Sample 2. Te (26.8 mg, 0.210 mmol, 77.3% ^{125}Te) and Se (87.2 mg, 1.10 mmol) were combined with AsF_5 (52 mg, 0.31 mmol) and AsF_3 (5 g) in a small glass vessel equipped with a magnetic stirring bar. The reaction mixture was stirred for 16 h. The resulting deep brown solution was then filtered through a glass frit into a 10-mm NMR tube and the tube was then flame sealed.

Nuclear Magnetic Resonance Spectroscopy. ^{77}Se NMR spectra were obtained with a Bruker WH-400 multinuclear spectrometer at 76.42 MHz in 16K of memory with a spectral width of 50 kHz (6.1 Hz/data point; pulse repetition time 0.16 s) and a pulse width of 40 μs. ^{125}Te NMR spectra were obtained with a Bruker WM-250 multinuclear spectrometer at 78.97 MHz in 16K of memory with spectral widths of 20–25 kHz (2.4–3.0 Hz/data point; pulse repetition time 0.41–0.33 s) and a pulse width of 20 μs. Samples were run unlocked (field drift <1 Hz/h) and referenced externally to saturated aqueous H_2SeO_3 and $Te(OH)_6$ at 25 °C. Spectra were simulated and summed with a Nicolet 1180 computer in the program NTCFT and plotted with a Zeta Plotter 100.

(1) Birchall, T.; Gillespie, R. J.; Vekris, S. L. *Can. J. Chem.* **1965**, *43*, 1672.
(2) Brevard, C.; Granger, P. "Handbook of High Resolution Multinuclear NMR"; Wiley: New York, 1981.
(3) McFarlane, C.; McFarlane, W. In "NMR and the Periodic Table"; Harris, P. K., Mann, B. E., Eds.; Academic Press: London, 1978; Chapter 12.
(4) Gillespie, R. J.; Passmore, J. *Chem. Br.* **1972**, *8*, 475.
(5) Boldrini, P.; Brown, I. D.; Gillespie, R. J.; Ireland, P. R.; Luk, W.-C.; Slim, D. R.; Vekris, J. E. *Inorg. Chem.* **1976**, *15*, 765.
(6) Gillespie, R. J.; Luk, W.-C.; Maharajh, E.; Slim, D. R. *Inorg. Chem.* **1977**, *16*, 892.
(7) Burns, R. C.; Gillespie, R. J.; Luk, W.-C.; Slim, D. R. *Inorg. Chem.* **1979**, *18*, 3086.
(8) Burns, R. C.; Chan, W.-L.; Gillespie, R. J.; Luk, W.-C.; Sawyer, J. F.; Slim, D. R. *Inorg. Chem.* **1980**, *19*, 1432.
(9) Lassigne, C. R.; Wells, E. J. *J. Chem. Soc., Chem. Commun.* **1978**, 956.
(10) Schrobilgen, G. J.; Burns, R. C.; Granger, P. *J. Chem. Soc., Chem. Commun.* **1978**, 957.
(11) Collins, M. J.; Gillespie, R. J.; Sawyer, J. F., submitted for publication.
(12) McMullan, R. K.; Prince, D. J.; Corbett, J. D. *Inorg. Chem.* **1971**, *10*, 1749.
(13) Burns, R. C.; Collins, M. J.; Gillespie, R. J.; Schrobilgen, G. J., unpublished results.
(14) Vogel, A. "A Textbook of Quantitative Inorganic Analysis", 4th ed.; Longmans, Green and Co.: London, 1978; p 478.

0020-1669/84/1323-1975$01.50/0